

GEOLOGY

## Two Genetic Types of Sericitolites in the Near-Polar Urals

I. V. Kozyreva, I. V. Shvetsova, and Ya. E. Yudovich

Presented by Academician N.P. Yushkin April 7, 2006

Received April 24, 2006

DOI: 10.1134/S1028334X07030075

Sericitolites are metamorphic and vein rocks that contain more than 50% sericite (a less common variety of muscovite). Therefore, these rocks are enriched in K ( $\geq 5\% K_2O$ ). We studied them in the following regions of the near-Polar Urals: the Maldynyrd Ridge (left bank of the Balban'yu River, the large left tributary of the Kozhim River), the Chernaya Gora Ridge sometimes outlined as the southern spur of the Rosomakha Ridge (left bank of the Kozhim River), and the Zhelannoe deposit (the largest vein quartz and rock crystal deposit in Europe). Although these regions are spaced at no more than 3 km along the Balban'yu River valley, we can recognize here two discrete (stratiform and vein) morphological types of sericitolite.

The *stratiform sericitolites* occur as beds (from 0.3 to 4.7 m thick) in the canyon of the Al'kesvozh Creek and the cirque of Lake Grubependity. The sericitolites are characterized by the presence of pyrophyllite, chloritoid, hematite, diaspore, and less common kyanite. The majority of sericitolites are apoarkosic schists, i.e., rocks formed after rhyolitic or arkosic rocks (the arkoses, in turn, developed after rhyolites). The rhyolites are considered Cambrian rocks (Rb–Sr age  $516 \pm 19$  Ma) [7, p. 12]. The apoarkosic schists are ascribed to the basal Al'kesvozh sequence of the Paleozoic (Upper Cambrian–Lower Ordovician) section [4].

The *vein sericitolites* occur in the study region at the outer contact of quartz veins with rock crystals (RC) in Lower Ordovician quartzite sandstones of the Obeiz (Telpos) Formation. Friable (leached) quartz–sericite rocks are described in several works [1, 2, 5, and others]. The dense sericitolites are developed in the lower parts of RC-bearing pockets in the Zhelannoe deposit [6].

In 1992–1999, we investigated sericitolites of both types. In the present paper, geochemical data reported in [3, 4] are supplemented with our original data on the geochemistry and mineralogy of these specific rocks of morphologically and genetically different types.

Application of the lithochemical method [8] using the hydrolyzate–titanium (HM–TM) module diagram makes it possible to distinguish five clusters and two domains (Fig. 1, Table 1).

The stratiform sericitolites make up three clusters and one domain with different amounts (HM module) and proportions of hydrolyzate components (TM and IM modules). Cluster I includes aporhyolitic sericitolites. Cluster II contains aporhyolitic sericitolites with hematite, diaspore, and kyanite (II). Cluster III includes hematite sericitolites. The domain is composed of chloritoid–sericite schists (sample 6851).

The vein sericitolites make up two clusters of rocks transformed by superimposed RC-forming processes into dense and friable varieties (clusters IV and V, respectively). They are characterized by very high contents of Ti (up to 11%  $TiO_2$ ). The friable sericitolite

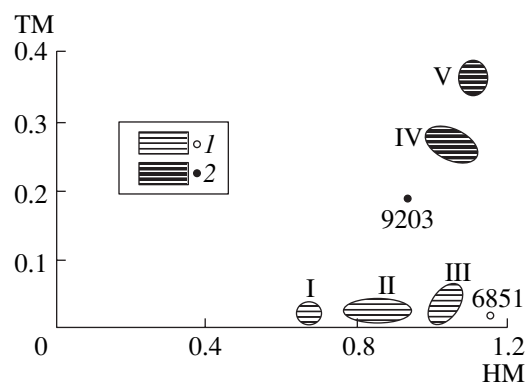


Fig. 1. The HM–TM module diagram. Sericitolites: (1) stratiform, (2) vein.

**Table 1.** Chemical composition of sericitolites, wt %

| Oxides and modules             | Stratiform sericitolites |        |       |       | Vein sericitolites |       |       |
|--------------------------------|--------------------------|--------|-------|-------|--------------------|-------|-------|
|                                | I                        | II     | III   | 6851  | IV                 | V     | 9203  |
|                                | Alkalites                |        |       |       | Ti-alkalites       |       |       |
| SiO <sub>2</sub>               | 51.65                    | 46.49  | 40.22 | 39.20 | 40.79              | 40.38 | 42.64 |
| TiO <sub>2</sub>               | 0.37                     | 0.55   | 0.84  | 0.38  | 8.08               | 10.10 | 5.92  |
| Al <sub>2</sub> O <sub>3</sub> | 31.18                    | 33.63  | 27.41 | 36.76 | 29.73              | 28.06 | 30.60 |
| Fe <sub>2</sub> O <sub>3</sub> | 2.57                     | 4.45   | 13.70 | 2.74  | 5.15               | 5.47  | 3.63  |
| FeO                            | 0.16                     | 0.16   | 0.35  | 5.57  | 0.13               | 0.23  | 0.32  |
| MnO                            | 0.01                     | <0.005 | 0.12  | 0.43  | <0.005             | 0.04  | 0.006 |
| MgO                            | 0.48                     | 0.29   | 2.05  | 0.31  | 0.79               | 1.24  | 1.10  |
| CaO                            | <0.1                     | 0.10   | 0.88  | 0.47  | 0.66               | 1.09  | 0.33  |
| Na <sub>2</sub> O              | 0.18                     | 0.70   | 0.23  | 0.74  | 0.65               | 0.44  | 0.68  |
| K <sub>2</sub> O               | 9.35                     | 8.53   | 9.52  | 7.72  | 8.93               | 7.64  | 8.96  |
| P <sub>2</sub> O <sub>5</sub>  | 0.04                     | 0.04   | 0.38  | 0.09  | 0.07               | 0.05  | 0.12  |
| L.O.I.                         | 3.77                     | 4.71   | 4.03  | 5.39  | 4.13               | 4.97  | 5.00  |
| Total                          | 99.72                    | 99.65  | 99.71 | 99.79 | 99.10              | 99.67 | 99.31 |
| HM                             | 0.66                     | 0.83   | 1.05  | 1.17  | 1.06               | 1.09  | 0.95  |
| TM                             | 0.012                    | 0.016  | 0.030 | 0.010 | 0.272              | 0.360 | 0.193 |
| IM                             | 0.09                     | 0.14   | 0.50  | 0.24  | 0.14               | 0.15  | 0.11  |
| AM                             | 0.31                     | 0.27   | 0.36  | 0.23  | 0.32               | 0.29  | 0.32  |
| Number of analyses             | 2                        | 5      | 2     | 1     | 2                  | 2     | 1     |

sample 9203 (located beyond the clusters in Fig. 1) is distinguished from rocks of clusters IV and V by lower HM and TM values and the lack of hematite.

Table 2 presents the comparative characteristics of accessory mineralization in sericitolites of both types. Microprobe analysis showed that the rock-forming sericites of both sericitolites have similar compositions. For example, the Fe<sub>2</sub>O<sub>3</sub> content is as high as 3–5% in the vein type and 5.92% in the stratiform type (sample 6131) [6]. The stratiform variety is characterized by a greater diversity of polygenous accessory components (joint presence of both allothigenic and neogenic minerals), whereas all (or nearly all) minerals of the vein variety probably represent authigenic species.

At present, detailed data are available only for the vein sericitolites first investigated by Repina [6].

**Zircon.** Sericitolites of the Zhelannoe deposit are characterized by a high content of zircon (0.6–2 wt %, average 1%) [6]. The zircon content does not exceed 50 g/t in the enclosing quartzite sandstones. The zircon grains can be divided into three morphological types: (1) rounded grains (~90 wt %, Fig. 2a); (2) faceted crystals with dissolution signs (~5 wt %); and (3) equant elongate-prismatic crystals (~5 wt %). We believe that the morphology of the rounded crystals is related to

processes of dissolution rather than rolling. All minerals of sericitolites were repeatedly subjected to dissolution [6]. In addition, the rounded morphology can also be related to growth from supersaturated solutions. According to [6], the rounded zircon is characterized by a fine zonal structure with a variable Hf content.

The well-crystallized *leucoxene*, often similar to the fine-crystalline rutile aggregate, can be a transitional variety of the neogenic rutile.

**Rutile** is a neogenic mineral developed as equant short- and long-prismatic crystals, as well as parallel intergrowths, cranked twins, and aggregates (Fig. 2b). **Tourmaline** (4–6%, up to 12% in some places [6]) occurs as equant long-prismatic and acicular crystals with numerous intergrowths (Fig. 2c). According to [6], the initial stage of vein quartz crystallization was marked by the formation of the colorless tourmaline that was later subjected to dissolution. The relict tourmaline grains served as seed for crystallization of the darker variety of the schorl–dravite series.

**Monazite** is surprisingly abundant (up to 2549 g/t [6]) in sericitolites developed near the RC-bearing patches in sterile quartzite sandstones of the Lower Ordovician Obeiz Formation. Monazite occurs as pale yellow (less commonly, reddish yellow) crystals of

**Table 2.** Comparative characteristics of accessory minerals in sericitolites (compiled by I.V. Shvetsova)

| Mineral                    | Vein sericitolites   | Stratiform sericitolites                                      |
|----------------------------|--|---|
| Leucoxene                  | Crystallized up to rutile aggregates (0.5–1.0)                               | Rounded grains without traces of recrystallization (0.01–0.5) |
| Rutile                     | Newly formed equant (0.01–0.1)   | Rare allothigenic grains (0.01–0.1)                           |
| Sphene                     | Rare crystals (0.01–0.5)   | Rare grains (0.01–0.5)  |
| Zircon                     | Mainly rounded grains (0.1–1.0)  | Rounded crystallites (0.01–0.1)                               |
| Apatite                    | Newly formed elongate-prismatic crystals (0.2–0.5)                           | Rare tabular crystals (0.01–0.5)                              |
| Monazite                   | Newly formed equant prismatic crystals (0.5–1.0) and occasional intergrowths | Oblate monazite 1 crystals (0.1–0.5) [3]                      |
| Xenotime                   | Equant dipyrarnidal and prismatic crystals (0.05–0.1)                        | Dark brown and milky white (?) grains (0.01–0.1)              |
| Chloritoid                 | Absent   | Equant tabular crystals (0.1–1.0)                             |
| Tourmaline                 | Newly formed equant elongate-prismatic crystals (0.4–5.0)                    | Rare crystallites (0.05–0.2)                                  |
| Barite                     | Equant tabular crystals with well-developed apices (0.1–0.5)                 | Grains (0.5–1.0)  |
| Florencite and svanbergite | Equant orthorhombic or pseudocubic crystals (0.01–0.1)                       | Poorly developed crystallites (0.01–0.5)                      |
| Kyanite                    | Absent   | Crystals (0.2–0.5)  |
| Diaspore                   | Absent   | Aggregates of lamellar crystals (0.1–0.5)                     |
| Euclase                    | Absent   | Prismatic crystals (0.1–0.2)                                  |
| Spessartine                | Absent   | Equant crystals (0.01–0.05)                                   |
| Allanite                   | Absent   | Grains (0.05–0.2)   |

Note: (r.g.) Rare grains. Grain and crystal size are given in parentheses (mm).

three morphological types: (1) long-prismatic crystals (the dominant type) up to 1 cm long (Fig. 2d); (2) tabular (slightly elongated) crystals with well-developed apices; and (3) parallel and sheaflike crystals. The crystals often contain rutile, hematite, and zircon inclusions. The presence of sheath-shaped crystals in some places suggests a unilateral influx of solution [6]. The abundance of split crystals indicates that they included numerous solid particles in the solution during their growth. The monazite crystals have an unusual composition: the LREE content is decreased relative to MREE and HREE [6].

*Xenotime* associated with monazite is a subordinate component that occurs as two morphological types: (1) poorly crystallized prismatic (sometimes elongate-prismatic xenotime 1) and (2) bipyramidal xenotime 2 with a narrow prismatic zone (Fig. 2f). According to [6], xenotime with the  $WO_3$  admixture (up to 2–3%) formed at the RC-bearing stage of the redistribution and mobilization of rare earth elements of the yttrium group in the course of the hydrothermal alteration of sericitolites.

In addition to the minerals mentioned above and shown in Table 2, fuchsite, sulfides, and native gold are also present in the vein sericitolites. The native gold was first detected in 1997 by V.S. Ozerov in the course of sampling mining gallery dumps. The panning of 1 m<sup>3</sup>

of rocks yielded 20 equant gold flakes (~0.2 mm in size) with fragments of edges. They do not make up intergrowths with other minerals [6].

The vein sericitolites are undoubtedly hydrothermal formations. This conclusion is supported by their morphology, association with quartz veins [1, 2], and confinement to the RC-bearing pockets in some cases. According to [6], these rocks are products of the two-stage crystallization of hydrothermal siliceous–alkaline solutions that also served as a source for quartz veins. The minerals precipitated in two stages. The first stage (tourmaline, zircon, rutile, hematite, monazite, and muscovite) was synchronous with the vein stage ( $T \approx 400^\circ\text{C}$ ,  $P = 150\text{--}350$  atm, and pH 7.2–8.0) of the sericitolite formation. The second stage (tourmaline 2, zircon 2, monazite 2, xenotime, fuchsite, and gold) was synchronous with the formation of RC-bearing pockets ( $T \approx 310^\circ\text{C}$ ,  $P = 100\text{--}150$  atm, and pH 7.0–7.5).

The stratiform sericitolites have a different genesis. They associate with the REE-bearing quartz–pyrophyllite and phengite–chloritoid–pyrophyllite schists and diasporites that correspond to the alteration series of rhyolites [4]. Therefore, the stratiform sericitolites can be interpreted as a part of the thermal endogenic (or primarily low-temperature exogenic) metasomatic column that represented an ancient weathering crust of rhyolites. We believe that the interrelations between

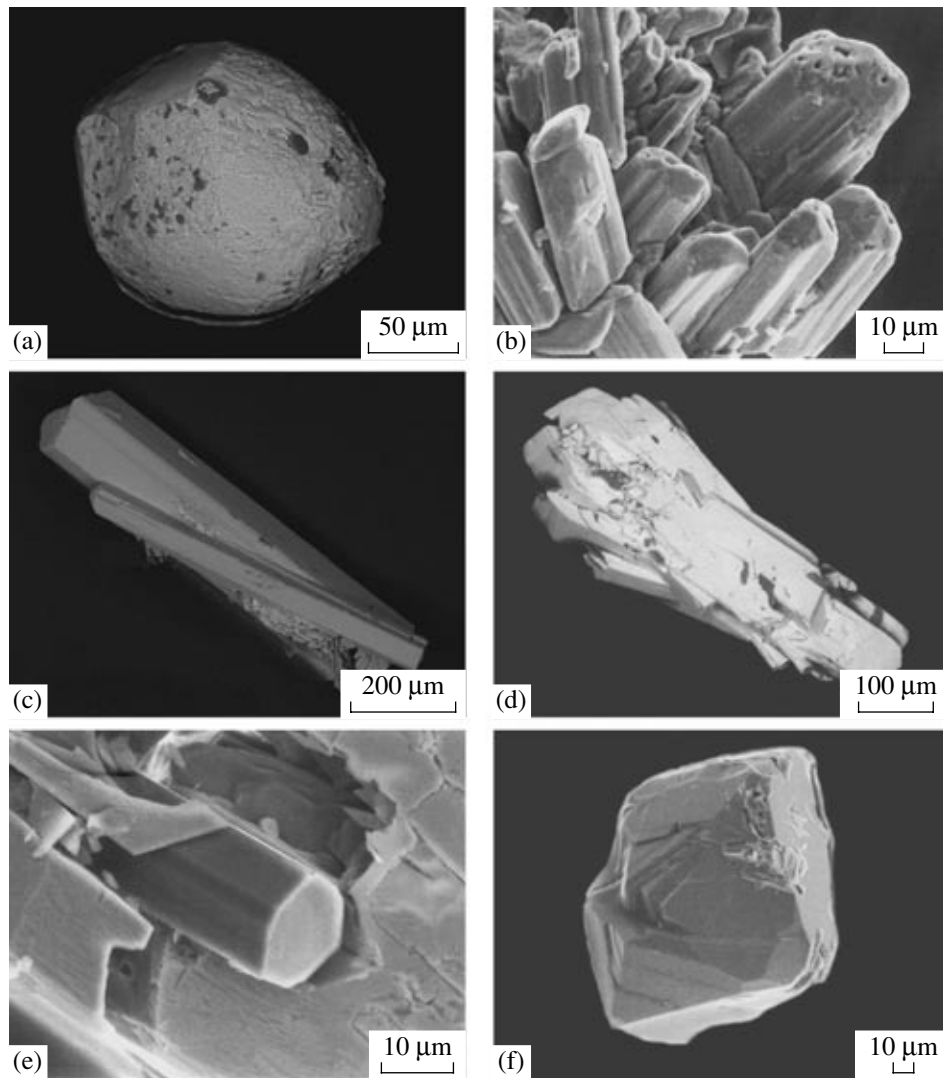


**Fig. 2.** Segregation mode of accessory minerals in vein sericitolites. (a) Rounded zircon crystal with fractured surface and leaching caverns (sample 9977); (b) rutile crystal aggregate with channels related to the rapid growth of crystals (sample 9974); (c) intergrowth of elongate-prismatic equant tourmaline crystals (sample 9977); (d) sheaflike aggregate of flattened elongate-prismatic monazite crystals (sample 9974); (e) elongate-prismatic monazite crystal (closeup of Fig. 2d); (f) dipyramidal xenotime crystal (sample 9202).

rocks in the weathering profile reported in [3, p. 61] fit the model of fault-line metasomatism rather than the weathering of rhyolites.

It is evident that further detailed comparative analyses of similar minerals (e.g., zircon, tourmaline, monazite, and rutile) from both sericitolite types are essential for more confident elucidation of the genesis of sericitolites discussed in this paper.

#### REFERENCES

1. V. V. Bukanov, *Rock Crystals in the Near-Polar Urals* (Nauka, 1974) [in Russian].
2. V. V. Bukanov, V. A. Bukanova, and N. D. Vasilevskii, in *Yearbook-1971* (Inst. Geol. Komi Fil. AN SSSR, Syktyvkar, 1972), pp. 152–157 [in Russian].
3. *Geochemistry of Ancient Sequences in the Northern Urals*, Ed. by Ya. E. Yudovich and M.P. Ketris (Geoprint, Syktyvkar, 2002) [in Russian].
4. Ya. E. Yudovich, L. I. Efanova, I. V. Shvetsova, et al., *Interformation Contact Zone in the Cirque of Lake Grubependity* (Geoprint, Syktyvkar, 2002) [in Russian].
5. A. E. Karyakin and V. A. Smirnova, *Structures of Rock Crystal Fields* (Nedra, Moscow, 1967) [in Russian].
6. S. A. Repina, *Geology and Mineral Resources of the European Part of Northeast Russia: New Results and Perspectives* (Syktyvkar, 1999), Vol. 4, pp. 105–108 [in Russian].
7. A. A. Soboleva, *Rhyolites of the Near-Polar Urals and the Southern Polar Urals* (Geoprint, Syktyvkar, 1995) [in Russian].
8. Ya. E. Yudovich and M. P. Ketris, *Principles of Lithochemistry* (Nauka, St. Petersburg, 2000) [in Russian].